INFECTION AND IMMUNITY, June 2008, p. 2273–2283 Vol. 76, No. 6
0019-9567/08/$08.00+0 doi:10.1128/IAI.00102-08

The *Chlamydia trachomatis* Plasmid Is a Transcriptional Regulator of Chromosomal Genes and a Virulence Factor▽†

John H. Carlson,[1]‡ William M. Whitmire,[1]‡ Deborah D. Crane,[1] Luke Wicke,[2] Kimmo Virtaneva,[2] Daniel E. Sturdevant,[2] John J. Kupko III,[2] Stephen F. Porcella,[2] Neysha Martinez-Orengo,[2] Robert A. Heinzen,[1] Laszlo Kari,[1] and Harlan D. Caldwell[1]*

Laboratory of Intracellular Parasites,[1] and Genomics Unit Research Technologies Section,[2] Rocky Mountain Laboratories, National Institute of Allergy and Infectious Diseases, National Institutes of Health, Hamilton, Montana 59840

Received 24 January 2008/Returned for modification 25 February 2008/Accepted 6 March 2008

Chlamydia trachomatis **possesses a cryptic 7.5-kb plasmid of unknown function. Here, we describe a comprehensive molecular and biological characterization of the naturally occurring plasmidless human *C. trachomatis* strain L2(25667R). We found that despite minimal chromosomal polymorphisms, the LGV strain L2(25667R) was indistinguishable from plasmid-positive strain L2(434) with regard to its in vitro infectivity characteristics such as growth kinetics, plaquing efficiency, and plaque size. The only in vitro phenotypic differences between L2(434) and L2(25667R) were the accumulation of glycogen granules in the inclusion matrix and the lack of the typical intrainclusion Brownian-like movement characteristic of *C. trachomatis* strains. Conversely, we observed a marked difference between the two strains in their abilities to colonize and infect the female mouse genital tract. The 50% infective dose of plasmidless strain L2(25667R) was 400-fold greater (4×10^6 inclusion-forming units [IFU]) than that of plasmid-bearing strain L2(434) (1×10^4 IFU). Transcriptome analysis of the two strains demonstrated a decrease in the transcript levels of a subset of chromosomal genes for strain L2(25667R). Among those genes was *glgA*, encoding glycogen synthase, a finding consistent with the failure of L2(25667R) to accumulate glycogen granules. These findings support a primary role for the plasmid in in vivo infectivity and suggest that virulence is controlled, at least in part, by the plasmid's ability to regulate the expression of chromosomal genes. Our findings have important implications in understanding a role for the plasmid in the pathogenesis of human infection and disease.**

The 15 serovars of *Chlamydia trachomatis* are divided into two distinct disease-causing pathobiotypes: trachoma and lymphogranuloma venereum (LGV) (46). Trachoma serovars are noninvasive and epitheliotropic and are further subdivided by disease outcome: blinding trachoma (serovars A to C) or nondisseminating sexually transmitted disease (serovars D to K) (18, 46). LGV serovars (L1, L2, and L3) are also sexually transmitted but are invasive, resulting in a disseminating infection of regional draining lymph nodes (47). All strains go through a similar but unique biphasic developmental cycle (29) starting with the metabolically inactive infectious elementary body (EB) that attaches to and enters host cells by phagocytosis (7). Within the EB-laden phagosome, termed the chlamydial inclusion, the EB differentiates into the noninfectious metabolically active reticulate body (RB). The RB multiply by binary fission and then redifferentiate back into infectious EB. Following cell lysis, or exclusion of the inclusion from viable cells (56), EB are released into the extracellular environment, where they reinitiate the infectious cycle.

A fundamental ambiguity of *C. trachomatis* biology is the association of a cryptic 7.5-kb plasmid of unknown function (33). The strong selection to maintain the plasmid by human chlamydial strains implies its importance in the pathogenesis of human infection or disease (13, 33). All plasmid-borne genes are transcribed (42, 43), and at least one protein (pgp3) was shown to be expressed (12). Plasmidless variants originating from laboratory strains (25) and naturally occurring clinical isolates (2, 16, 24, 35, 52) have been identified and partially characterized. No significant differences in antibiotic sensitivity between isogenic plasmid-containing strains and plasmid-lacking strains were found (27, 28). A single and consistent phenotype identified for all *C. trachomatis* plasmidless isolates is their inability to accumulate glycogen in the inclusion (25). Neither the molecular basis for this association nor its potential role in the pathogenesis of human infection or disease is known.

All chlamydial species sequenced to date have the same complement of genes involved in glycogen metabolism, and all genes are chromosomally localized (3, 10, 20, 36, 39, 40, 50, 51, 54, 55). Fructose-6-phosphate is converted to glucose-1-phosphate through glucose-6-phosphate isomerase (*pgi*) and phosphoglucomutase (*mrsA_1*). Glucose-1-phosphate is then converted to ADP-glucose, the building block for glycogen synthesis, a reaction carried out by the gene product of *glgC*. Glycogen synthase (*glgA*) converts ADP-glucose to the linear glucose polymer (α-1,4-polyglucosyl chain), while the branching enzyme encoded by *glgB* forms the branched α-1,4-α-1,6-glucan polysaccharide (i.e., glycogen). Finally, the gene products of *glgX* (debranching enzyme) and *glgP* (glycogen phosphorylase)

* Corresponding author. Mailing address: Laboratory of Intracellular Parasites, Rocky Mountain Laboratories, National Institute of Allergy and Infectious Diseases, National Institutes of Health, 903 South 4th Street, Hamilton, MT 59840. Phone: (406) 363-9333. Fax: (406) 363-9380. E-mail: hcaldwell@niaid.nih.gov.

† Supplemental material for this article may be found at http://iai.asm.org/.

‡ J.H.C. and W.M.W. contributed equally to this work.

▽ Published ahead of print on 17 March 2008.

are responsible for glycogen catabolism. Interestingly, while all chlamydial species have the ability to synthesize glycogen, only *C. trachomatis* and *Chlamydia muridarum* have been shown to accumulate glycogen in the inclusion (17). In *C. trachomatis*, this difference in the ability to accumulate glycogen does not appear to be the result of differential expression levels of the glycogen metabolic genes (19). However, similar studies have not been conducted on plasmid-free variants.

C. muridarum (MoPn) is a mouse pathogen that shares a significant degree of genomic synteny, sequence identity, and biology with *C. trachomatis* (39). MoPn also possesses a related 7.5-kb cryptic plasmid that shares 80% nucleotide sequence identity to the *C. trachomatis* plasmid (39). Like *C. trachomatis*, MoPn inclusions stain positive for glycogen (31). The genetic relatedness, shared biology, conservation of a cryptic plasmid, and availability of a MoPn small-animal model whose infection characteristics closely mimic those of human infection make this strain very attractive for characterizing a role for the cryptic plasmid in pathogenesis. To that end, O'Connell and Nicks (31) successfully cured MoPn of its cryptic plasmid by novobiocin treatment. The MoPn plasmid-free strain did not stain positive for glycogen and grew in cell culture with kinetics similar to those of wild-type MoPn but, importantly, did produce much smaller plaques than did plasmid-positive organisms (31). Interestingly, although the plasmid-negative strain was as infectious for mice as the plasmid-positive strain, it failed to elicit upper genital tract pathology despite comparable infectious loads in these tissues (30). This rather unusual finding has significant implications in defining a functional role for the plasmid in vivo, as it implicates a unique interaction with innate immunity mediators that might drive damaging inflammatory responses. However, the MoPn strain is not a human pathogen, and there was no description of the genetic relatedness between the novobiocin plasmid-cured and parental plasmid-positive strains. Thus, it remains unclear how the MoPn findings relate to the biology and pathogenesis of the naturally occurring plasmid-free human strains and the human host. We therefore believed that it was important to conduct a similar biological characterization of a naturally occurring *C. trachomatis* plasmidless strain whose complete genetic makeup was known.

Here, we describe a comprehensive biological, pathogenic, and genetic characterization of plasmid-bearing strain L2 (434) and the naturally occurring plasmidless LGV strain L2(25667R) (35) with the goal of understanding the role of the cryptic plasmid in *C. trachomatis* pathogenesis. We present evidence showing that these two strains exhibit similar in vitro virulence characteristics but differ markedly in their in vivo virulence properties. Interestingly, this distinction in virulence was not associated with significant chromosomal changes but was associated with differential transcript levels of specific chromosomal genes. These findings imply an important role for the cryptic plasmid in the pathogenesis of *C. trachomatis* infection of humans.

MATERIALS AND METHODS

Chlamydiae. *C. trachomatis* reference strain L2(434) (L2/LGV-434/Bu) and L2(25667R) (35) EB were purified from infected HeLa 229 cells by density gradient centrifugation, aliquoted, and stored at −80°C as previously described (8). Strain L2(25667R) was originally isolated by Schachter and Osoba (49) and kindly provided by Luis de la Maza (University of California, Irvine, CA).

One-step growth curves. Mouse McCoy cells were aliquoted in 24-well (2.5×10^5 cells/well) flat-bottomed tissue culture-treated plates (Corning, Inc., Corning, NY) and inoculated with L2(434) or L2(25667R) cells suspended in a 0.2-ml solution containing 10 mM phosphate, 250 mM sucrose, and 5 mM glutamic acid (pH 7.2) at a multiplicity of infection (MOI) of 0.5. The plates were centrifuged for 1 h at $550 \times g$ and rocked at 37°C for 30 min. The inoculum was removed, and monolayers were washed with Hanks balanced salt solution; fed with 1 ml of Dulbecco's modified Eagle's medium (Mediatech, Inc., Herndon, VA) containing 4.5 mg/ml glucose, 2 mM L-glutamine, 1 mM HEPES, 1 mM sodium pyruvate, 0.055 mM β-mercaptoethanol, 10% fetal bovine serum, 10 μg/ml gentamicin, and 1 μg/ml cycloheximide (DMEM10); and incubated at 37°C in an atmosphere of 95% air and 5% CO_2. At 6, 12, 24, 28, 32, 36, 40, and 48 h postinfection (p.i.), infected cells were harvested in a 0.2-ml solution containing 10 mM phosphate, 250 mM sucrose, and 5 mM glutamic acid and mechanically disrupted by sonication, and recoverable inclusion-forming units (IFU) were counted (45).

Plating efficiency. L2(434) and L2(25667R) cells were grown in 24-well McCoy monolayers as described above. Replicate plates were centrifuged for 1 h at room temperature, followed by rocking for 30 min at 37°C, or were rocked without centrifugation for 30 min. Infected monolayers were then fed with DMEM10 with or without cycloheximide (1 μg/ml). The monolayers were fixed with methanol 24 h p.i., and IFU were enumerated. Each experiment was conducted in duplicate.

Plaquing efficiency. L2(434) and L2(25667R) were evaluated for their rates of plaque formation and plaque sizes by infecting six-well McCoy monolayers as described previously by Matsumoto et al. (25). Monolayers were stained with neutral red at 5, 7, 9, 11, and 13 days p.i. and examined for plaques. Plaques from each strain at the various times p.i. were enumerated and comparatively evaluated for morphology and size.

Glycogen staining. Monolayers of McCoy cells grown in 24-well plates were infected with L2(434) and L2(25667R) at an MOI of 0.3. Infected cultures were incubated at 37°C for 40 h, the growth media were removed, and the monolayers were allowed to completely air dry at room temperature. Monolayers were then fixed in absolute methanol for 10 min and sequentially stained by indirect immunofluorescence (indirect immunofluorescence assay [IFA]) or iodine (48). IFA staining was done using monoclonal antibody L2-145 (anti-L2 major outer membrane protein [MOMP]) or monoclonal antibody EV1-H1 (anti-lipopolysaccharide [LPS]), followed by Alexa Fluor 488-labeled goat anti-mouse immunoglobulin G secondary antibody (Invitrogen, Carlsbad, CA) as previously described (34).

Microscopy and live-cell imaging. For phase-contrast microscopy and live-cell imaging, subconfluent monolayers of McCoy cells in 35-mm glass-bottom culture dishes containing size #0 cover glasses (MatTek Corp., Ashland, MA) were infected with L2(434) or L2(25667R) cells at an MOI of 0.1 by rocking for 2 h at 37°C. Infected monolayers were fed with 3 ml of DMEM10 containing 1 μg/ml cycloheximide and incubated for 40 h at 37°C in an atmosphere of 95% air–5% CO_2. Digital time-lapse videos of infected cells were obtained using a Nikon TE-2000 E (Nikon Instruments, Inc., Melville, NY) inverted microscope equipped with a CoolSNAP HQ digital camera (Roper Scientific, Tucson, AZ) and Metamorph software (Universal Imaging, Downington, PA). Phase-contrast images at a magnification of ×1,000 were collected at 0.5-s intervals. Resulting image stacks were processed using ImageJ software (written by Wayne Rasband at the National Institutes of Health and available by anonymous FTP [http://rsb.info.nih.gov/ij/]) and converted into QuickTime movies (Apple Computer, Inc., Cupertino, CA). Infected McCoy cells grown on 13-mm Thermonox plastic coverslips were fixed and processed for transmission electron microscopy (TEM) as described previously by Kennedy et al. (22). Silver proteinate staining was done as described previously by Chiappino et al. (11).

In vivo infectivity. Female C3H/HeJ mice were obtained from Jackson Laboratories (Bar Harbor, ME). Groups of six mice each were inoculated vaginally with 5-μl aliquots of 10-fold serial dilutions of L2(434) or L2(25667R) EB ranging from 1×10^1 to 1×10^7 IFU. Mice were injected with medroxyprogesterone acetate 10 and 3 days prior to infection as previously described (34). Vaginal swabs were taken at 3, 7, 14, 21, and 28 days postinoculation and cultured on monolayers of McCoy cells, and recoverable IFU were determined as described previously (34). The 50% infective dose (ID_{50}) of each strain was calculated as described previously by Reed and Muench (41).

Genomic DNA sequence analysis. Genomic DNA was purified for sequencing as previously described (10). Ten micrograms of genomic DNA was subjected to genomic mutation mapping and resequencing (Nimblegen Systems, Inc.) as previously described (21).

PCR and nucleic acid purification for quantitative analysis. Chlamydial genomic DNA for PCR amplification was isolated as previously described (9). Plasmid-specific PCR primers (35) were used to detect plasmid DNA in L2(434)

TABLE 1. Single-nucleotide polymorphisms identified in L2(25667R) versus L2(434)[a]

ORF	nt mutation	aa substitution	Predicted function
CTL0043	C>T	P54L	*gspD yscC*
CTL0314	C>A	A92S	Unknown
CTL0885/CTL0886	C>T	Intergenic	Unknown

[a] nt, nucleotide; aa, amino acid.

and L2(25667R) cultures through the use of the Expand High Fidelity PCR system (Roche Applied Science, Indianapolis, IN). For quantitative reverse transcription-PCR (qRT-PCR), TRIzol (Invitrogen)-extracted RNA was isolated from replicate monolayers of L2(434)- and L2(25667R)-infected cells (MOI of 1) grown on six-well flat-bottom plates (Costar; Corning Inc.) for 8, 12, 16, 24, 32, and 40 h p.i. Total DNA was similarly isolated from biological replicate cultures using an UltraClean microbial DNA isolation kit (Mo Bio Laboratories, Carlsbad, CA). Quantitative PCR was conducted on the purified genomic DNA using an *rpoB*-specific primer and probe set, and DNA concentrations were converted to copy numbers using the molecular mass of the bacterial genome (51). The primer and probe sequences are listed in Table S1 in the supplemental material. All quantitative amplifications were conducted as described below.

Microarray. Eighteen T75 flasks containing McCoy cells (4×10^7 cells) were divided into three groups (six each) and infected with L2(434) or L2(25667R) (MOI of 1) or mock infected and grown for 24 h at 37°C with 5% CO_2. The medium was removed by aspiration, and 5 ml of RLT Plus buffer (Allprep 96-well kit; Qiagen, Valencia, CA) was added to each flask in randomized order. Both DNA and RNA were simultaneously extracted from all 18 samples using the Allprep 96-well kit (Qiagen) according to the manufacturer's specifications. Contaminating DNA was removed from all RNA samples as described previously (59). RNA samples were converted to cDNA, biotinylated, and hybridized to gene chip arrays as described previously (15, 59).

Affymetrix GeneChip array. The custom array was designed using open reading frames (ORF) of *C. trachomatis* A/HAR-13 (10), with the L2(434) ORF (as annotated by Integrated Genomics, Chicago, IL) (97% or less DNA sequence identity against A/HAR-13 ORF) (54) included. The Affymetrix GeneChip RMLChip 3a (Gene Expression Omnibus accession number GPL4692), contains 97.8% coverage of the genome from L2(434) (938 probe sets of 959 ORF), resulting in a total of 9,506 perfectly matched probes.

Microarray data analysis. Affymetrix (Santa Clara, CA) GeneChip operating software, version 1.4, was used to perform the preliminary analysis. All *.CEL files were scaled to a trimmed mean of 500 using a scale mask for the L2 probe sets in order to create the *.CHP files. A pivot table from the *.CHP files was used to perform hierarchical clustering using a Pearson correlation similarity measure with average linkage and GeneSpring GX software, version 7.3 (data not shown). Quantile normalized values were subjected to a principal-component analysis (Partek Inc., St. Louis, MO). The false discovery rate (FDR) was determined for the *P* values in order to correct for multiple testing. Analysis of variance (ANOVA) (Partek Inc.) was determined for treatment [L2(25667R) versus L2(434) as a categorical factor]. ANOVA *P* values were filtered using the FDR cutoff of 0.0133. Gene lists were generated as described previously (23, 32). To be included in the final gene list, values were analyzed by ANOVA, significance analysis of microarrays (FDR of ≤0.29%) (57), a Student's *t* test (*P* value of ≤0.05), signal above background, and call consistency of ≥90%, and a twofold or higher minimum threshold filter was applied.

qRT-PCR validation of microarray data. qRT-PCR validation of GeneChip results was performed as described previously (59). RNA and genomic DNA were extracted from the same samples used for the microarray studies. mRNA signals were normalized to genomic DNA signals using the comparative threshold cycle method described previously (59). The primer and probe sequences for the target transcripts are listed in Table S1 in the supplemental material.

Microarray data accession number. Microarray data were submitted to the Gene Expression Omnibus database (www.ncbi.nim.nih.gov/geo) under accession number GSE10199.

RESULTS

Genomic sequencing of L2(25667R). PCR analysis on strain L2(25667R) resulted in no plasmid-specific products (data not shown), consistent with the findings previously described by Peterson et al. (35). The L2(25667R) genome was then sequenced using the microarray-based comparative genome sequencing strategy (1). This comparison revealed a surprisingly limited number of genomic differences between L2(25667R) and L2(434) (Table 1). Genomic changes in L2(25667R) were restricted to three single-nucleotide polymorphisms, two of which were found within ORF (CTL0043 and CTL0314), with the third located in an intergenic region upstream of ORF CTL0885 (Table 1). The two amino acid substitutions identified are relatively conservative and unlikely to alter protein function. This comparative sequence analysis of the two strains is essential for the in vitro and in vivo characterization studies that follow, as it ensures with a high level of confidence that the phenotypic differences between the strains can be ascribed to the presence or absence of the plasmid.

In vitro infectivity comparisons between L2(434) and L2(25667R). There have been no biological or genetic studies performed on plasmid-free strain L2(25667R) that would yield information regarding the role of the plasmid in the pathogenesis of human infection and disease. We believe these studies to be important, and we therefore undertook a detailed comparative characterization of strains L2(434) and L2(25667R). We first performed one-step growth curves, assayed plaque-forming kinetics and size, as well as studied the effects of centrifugation and inhibition of host protein synthesis on plating efficiencies of the organisms. The two strains were virtually indistinguishable from one another in every aspect of this comparative analysis. The strains grew at nearly identical rates following infection of McCoy cells (Fig. 1). We found no differences between the strains in their plaquing kinetics or plaque sizes (Fig. 2). Both strains generated visible plaques at day 7 p.i., and the plaque sizes of each strain were identical, ranging in diameter from 0.15 to 0.20 mm. Moreover, we observed no differences in the plating efficiencies between L2(434) and L2(25667R) when infections were performed with or without centrifugation of the inocula onto cell monolayers or when propagated in the presence or absence of the eukaryotic protein synthesis inhibitor cycloheximide (Table 2).

Glycogen accumulation differs between L2(434) and L2 (25667R) inclusions. Matsumoto et al. (25) previously reported

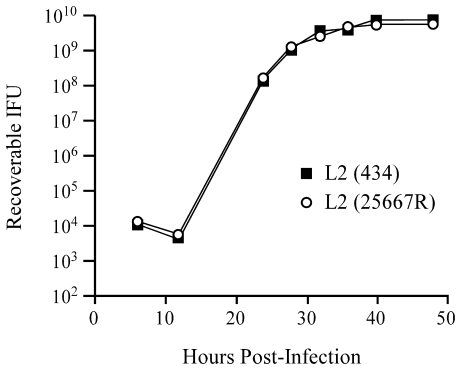

FIG. 1. L2(434) and L2(25667R) exhibit similar growth kinetics. One-step growth curves were conducted in McCoy cells infected with L2(434) or L2(25667R) at an MOI of 0.5, and recoverable IFU were determined at various times p.i. Each time point represents mean recoverable IFU from duplicate cell cultures.

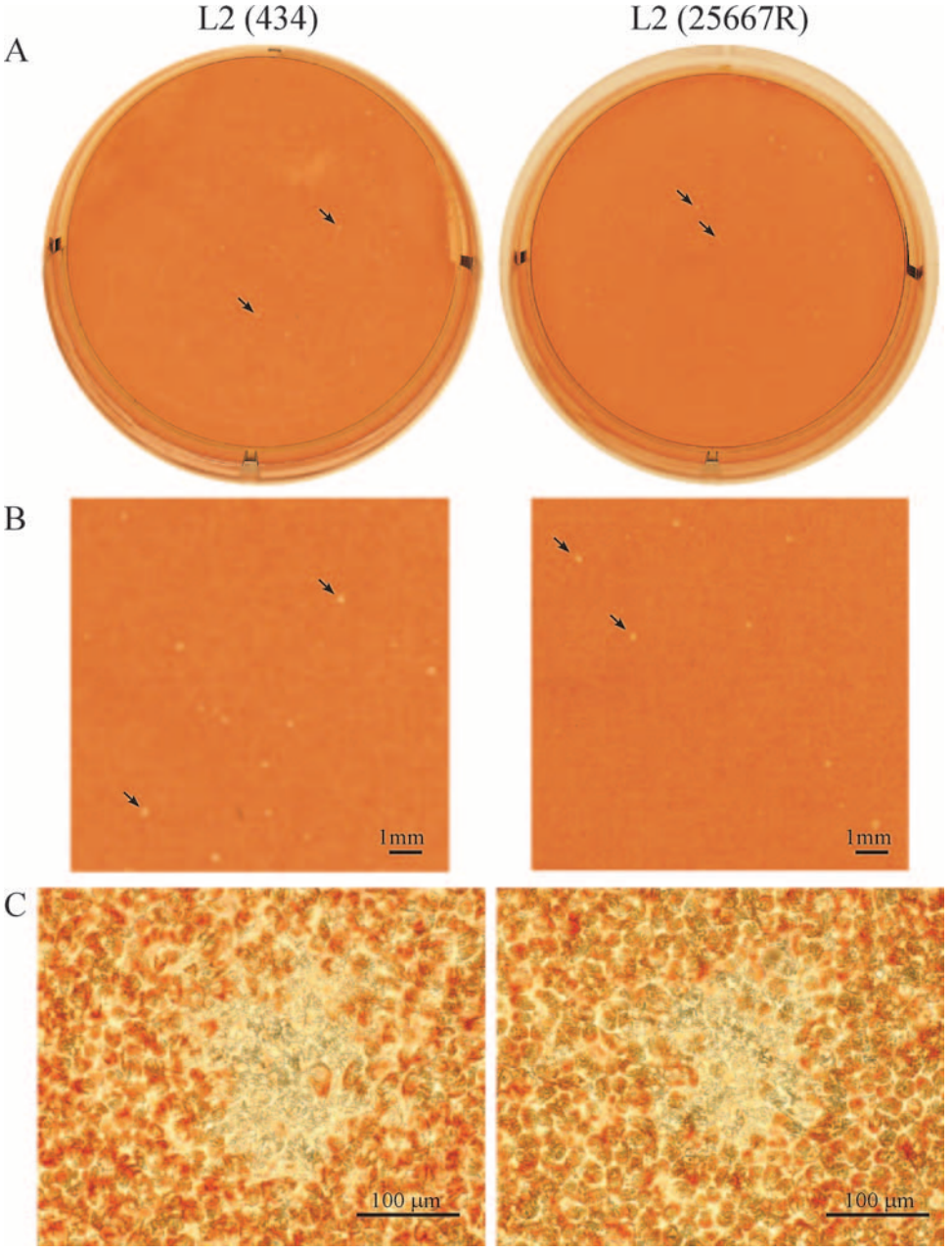

FIG. 2. L2(434) and L2(25667R) have similar plaque morphologies. McCoy cells grown in six-well plates were infected with L2(434) or L2(25667R) at approximately 200 IFU/well and neutral red stained for plaques at day 7. (A) Photograph of plaques taken from single wells of a six-well plate. (B) Macroscopic images of L2(434) and L2(25667R) plaques. (C) Microscopic images of L2(434) and L2(25667R) plaques.

that inclusions of *C. trachomatis* plasmidless variants were glycogen negative, as they failed to stain with iodine and lacked the intrainclusion electron-dense granules that Chiappino et al. (11) previously identified as being glycogen by silver proteinate staining. We therefore tested whether inclusions of L2(25667R) were devoid of glycogen. L2(434)- and L2(25667R)-infected McCoy cells were stained by IFA or with iodine. Inclusions of both strains stained positive by IFA (Fig. 3A and A′), but only inclusions of strain L2(434) stained with iodine (Fig. 3B and B′). We next examined these strains by TEM using fixation and poststaining methods capable of detecting glycogen granules. As shown in Fig. 4, L2(434) inclusions contained electron-dense particles (Fig. 4A) that stained intensely with silver proteinate (Fig. 4B). In contrast, the L2(25667R) inclusions lacked the electron-dense granules (Fig. 4A′). The predominance of the silver proteinate staining granules in the inclusion lumen of strain L2(434) is shown in Fig. 4C. These granules were absent in the inclusions of strain L2(25667R) (Fig. 4B′) but were occasionally detected in individual developmental forms (Fig. 4C′). These results are in agreement with data from the biochemical assays described previously by Matsumoto et al. (25), which demonstrated that the inclusions of a plasmidless isolate are not completely devoid of glycogen but

TABLE 2. Plasmid loss does not impair plating efficiency of *C. trachomatis*[a]

Strain	Expt	Plating efficiency (IFU)			
		With centrifugation		Without centrifugation	
		With cycloheximide	Without cycloheximide	With cycloheximide	Without cycloheximide
L2 (434)	1	3.76×10^{10}	3.55×10^{10}	4.16×10^{9}	3.73×10^{9}
	2	3.49×10^{10}	3.65×10^{10}	4.68×10^{9}	4.56×10^{9}
L2 (25667R)	1	4.20×10^{9}	3.20×10^{9}	3.49×10^{8}	2.87×10^{8}
	2	3.66×10^{9}	3.16×10^{9}	2.23×10^{8}	1.93×10^{8}

[a] The inocula for the strains were not standardized to contain the same IFU titers. The starting infectious load for the two strains differed by ~10-fold.

contain dramatically reduced levels compared to those of its parental (plasmid-positive) strain.

L2(25667R) exhibits distinct late-infection morphological features. With the exception of glycogen accumulation, the only other distinguishing feature that we observed between strains L2(434) and L2(25667R) was in inclusion morphogenesis and activity. Phase microscopy of cells at 40 h p.i. showed a marked difference in inclusion morphogenesis between the two strains (Fig. 5C and C′). The chlamydiae within L2(434) inclusions exhibited the characteristic *C. trachomatis* Brownian-like motility (see Video S1 in the supplemental material), and cell density was uniform throughout the inclusion (Fig. 5C). In contrast, L2(25667R) inclusions were morphologically unique, exhibiting little chlamydial intravacuolar motility (see Video S2 in the supplemental material). The inactive L2(25667R) inclusion contents exhibited a central dense amorphous structure surrounded by empty space that appeared to be devoid of organisms (Fig. 5C′). These structural features were not as apparent following IFA staining of the inclusions with anti-MOMP (Fig. 5A and A′) or LPS (Fig. 5B and B′) antibodies, but L2(25667R) inclusions tended to be smaller and stained less uniformly than those of the L2(434) strain. These marked morphological features of the inclusion contents did not change the infectious yield of strain L2(25667R) (Fig. 1). Moreover, TEM ultrastructural analysis of strain L2(25667R) showed typical developmental EB and RB forms similar to those found in strain L2(434) (Fig. 4). The inability of L2(25667R) inclusions to accumulate glycogen late in the infection was the only biological correlate of this atypical inclusion morphology.

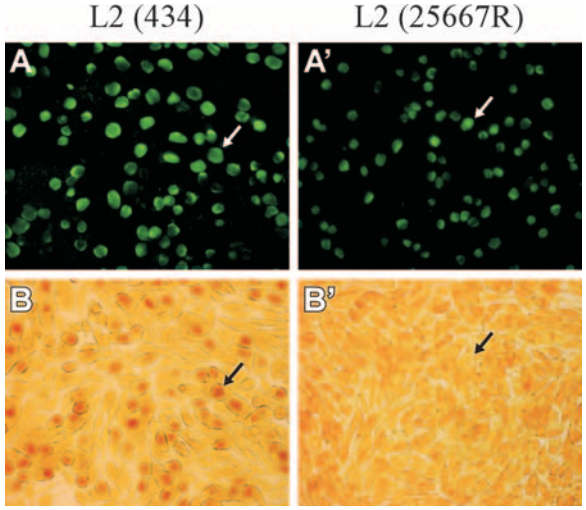

FIG. 3. L2(434) but not L2(25667R) inclusions stain positive for glycogen. McCoy cells were infected with L2(434) or L2(25667R) at an MOI of 0.3, fixed at 40 h p.i., and stained for MOMP. The same wells were subsequently stained for glycogen using the iodine staining technique. White arrows in the top panels indicate MOMP staining of individual inclusions of L2(434) (A) and L2(25667R) (A′), while black arrows in the bottom panels (B and B′) identify the same inclusions stained with iodine.

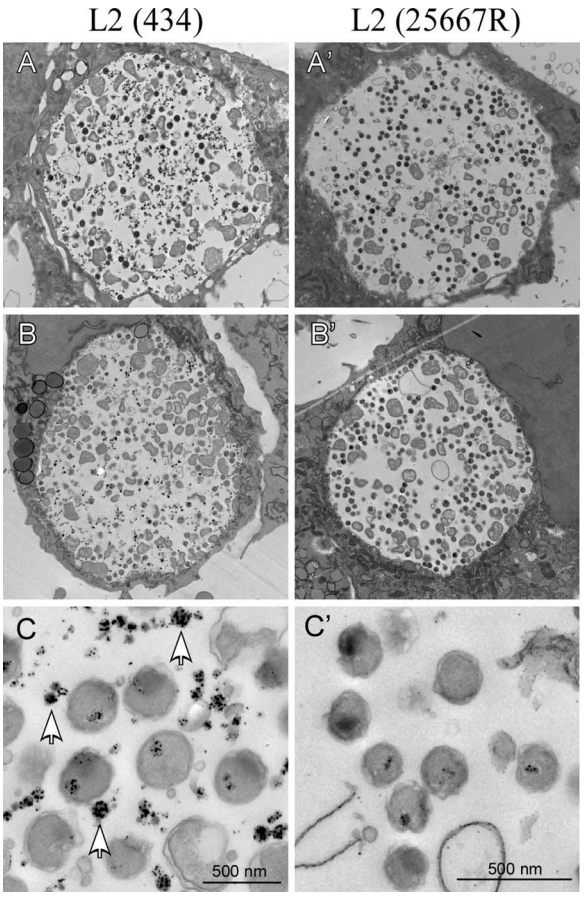

FIG. 4. Glycogen localizes to the lumen of mature L2(434) inclusions. Thin sections of L2(434) and L2(25667R) inclusions at 40 h p.i. are shown. (A and A′) Electron-dense extracellular material is present in the L2(434) (A) inclusion but not the L2(25667R) (A′) inclusion. (B and B′) Silver proteinate staining confirms that the electron-dense staining present in the L2(434) inclusion lumen (B) is glycogen, which is absent in the L2(25667R) inclusion (B′). (C and C′) Localization of silver on extracellular material by silver proteinate staining (arrows) indicates the presence of glycogen only in the lumen of the L2(434) (C) and not the L2(25667R) (C′) inclusions.

Determination of the ID_{50} values of L2(434) and L2(25667R) for the female mouse genital tract. Female C3H/HeJ mice (six per group) were inoculated intravaginally with 10^1, 10^2, 10^3, 10^4, 10^5, 10^6, or 10^7 IFU of L2(434) or L2(25667R). Infection was determined by culturing chlamydiae from cervicovaginal swabs on monolayers of McCoy cells at different times postinfection (Table 3). The ID_{50} for each strain was determined from the day 3 culture groups that had been intravaginally

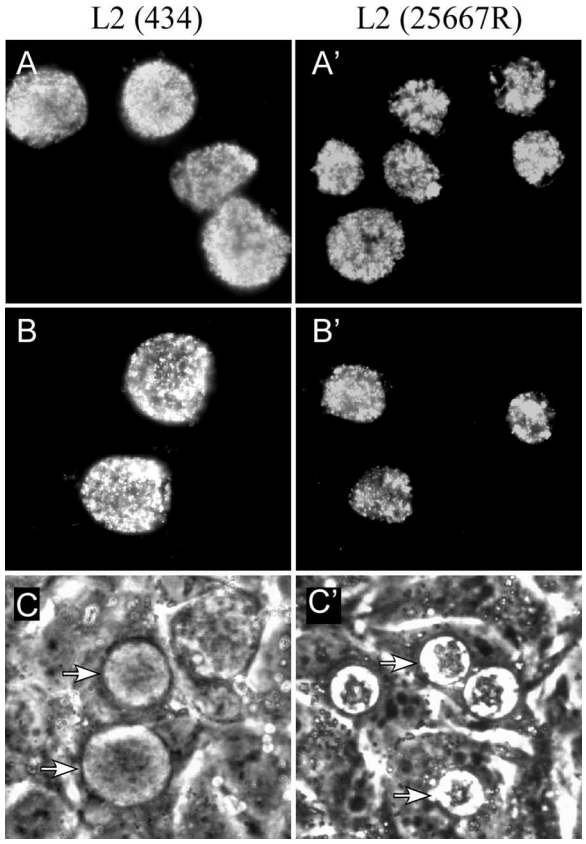

FIG. 5. Mature L2(434) and L2(25667R) inclusions are morphologically distinct by phase microscopy. (A to B′) Methanol-fixed inclusions following staining of McCoy cells for MOMP (A and A′) or LPS (B and B′) at 40 h p.i. (magnification, ×600). (C and C′) McCoy cell monolayers were infected at an MOI of 0.3 and viewed live after 40 h p.i. (magnification, ×400). Arrows indicate mature inclusions.

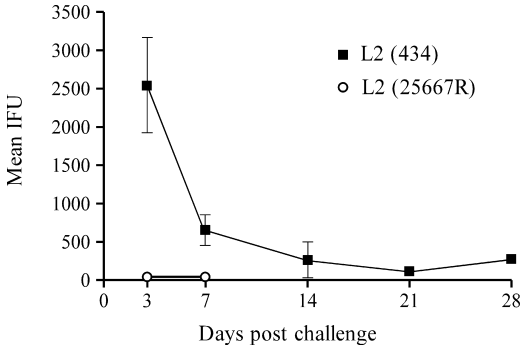

FIG. 6. L2(25667R) exhibits a decreased duration of infection compared to that of L2(434) in a murine model of infection. Shown are mean recoverable IFU values for culture-positive female C3H/HeJ mice challenged with 10^7 IFU of strain L2(434) or L2(25667R) as shown in Table 3. The actual mean recoverable IFU values for L2(25667R) on days 3 and 7 are 68 and 60, respectively. Error bars represent standard errors of the means.

challenged with different IFU. The ID_{50} of L2(434) was 1×10^4 IFU, whereas the ID_{50} of L2(25667R) was 4×10^6 IFU, a 400-fold difference. As importantly, mice infected with L2(434) shed significantly more infectious organism than did L2(25667R)-infected mice at all culture-positive periods following challenge (Fig. 6). Although L2(25667R) mice were culture positive at days 3 and 7 p.i., the recoverable IFU were 10- to 37-fold less than those of L2(434)-infected mice. L2(434)-challenged mice shed infectious organisms through day 28 p.i., whereas L2(25667R)-infected mice had resolved infection by day 14 p.i. These findings provide unambiguous evidence that the cryptic plasmid plays a critical role in the in vivo pathogenesis of *C. trachomatis* infection. They also strongly link the plasmid to the expression of virulence factors that function in the organism's ability to successfully colonize epithelial cells in vivo as well as in sustaining the infection once it is established. These findings encouraged us to further investigate the molecular basis for the plasmid's role in *C. trachomatis* pathogenesis. As our only biological link to these observed differences in in vivo pathogenesis was the in vitro differential intrainclusion accumulation of glycogen granules between the strains, we took a molecular approach in an attempt to define this potentially interesting relationship.

Glycogen accumulation is associated with *glgA* transcript levels. The genes involved in the glycogen metabolic pathway of *C. trachomatis* are shown in Fig. 7 (10, 51, 54). From our comparative genomic analysis, we knew that none of these genes differed between the two strains. Therefore, differences in glycogen accumulation might be a result of transcriptional differences between the two strains. qRT-PCR was performed on the five genes of this pathway to determine if there was a correlation between gene transcript levels and glycogen production between strains L2(434) and L2(25667R). We also analyzed transcript levels of candidate genes involved in the

TABLE 3. Determination of ID_{50} for L2(434) and L2(25667R) following intravaginal challenge of female C3H/HeJ mice[a]

Challenge dose (IFU)	No. of culture-positive mice per group at different times postchallenge/total no. of mice for strain:									
	L2(434) on day:					L2(25667R) on day:				
	3	7	14	21	28	3	7	14	21	28
10^7	6/6	6/6	2/6	2/6	1/6	5/6	4/6	0/6	0/6	0/6
10^6	5/6	5/6	3/6	3/6	3/6	0/6	0/6	0/6	0/6	0/6
10^5	5/6	2/6	2/6	0/6	0/6	0/6	1/6	0/6	0/6	0/6
10^4	4/6	1/6	0/6	0/6	0/6	0/6	1/6	0/6	0/6	0/6
10^3	0/6	0/6	ND	ND	ND	0/6	0/6	ND	ND	ND
10^2	0/6	0/6	ND	ND	ND	0/6	0/6	ND	ND	ND
10^1	0/6	0/6	ND	ND	ND	0/6	0/6	ND	ND	ND

[a] The ID_{50} was calculated as described in Materials and Methods using infected animals at day 3 postchallenge. ND, not done (cultures were not done on groups challenged with 10^1 to 10^3 IFU that exhibited two successive culture-negative swabs). Days 3, 7, 14, 21, and 28 indicate days postchallenge.

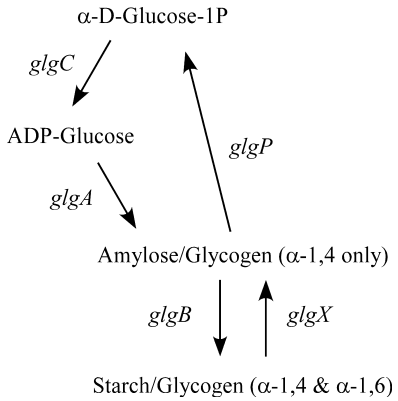

FIG. 7. Reaction scheme for glycogen metabolism in *C. trachomatis*.

earlier stages of glycogen biosynthesis, specifically, *pgi* and *mrsA_1*. Gene expression was analyzed for both strains temporally, ranging from 8 to 40 h p.i. Transcripts were normalized to genome copy number. Figure 8A demonstrates that the genome copy numbers for both strains were nearly identical for each time point p.i. The copy number also closely paralleled the recoverable IFU for each strain shown in the one-step growth curves (Fig. 1). The temporal changes in transcript levels of the *glg* genes for strains L2(434) and L2(25667R) are shown in Fig. 8B to F. The differential in *glgA* transcript levels between the two strains was significant at the 24-h (270-fold), 32-h (167-fold), and 40-h (57-fold) time points p.i. These findings corroborate the findings described previously by Belland et al. (5), who analyzed the transcriptome of the *C. trachomatis* growth cycle and identified *glgA* as being a late gene. Moreover, the expression of *glgA* directly correlates with the production and accumulation of glycogen late in the growth cycle of L2(434) and, conversely, the lack of glycogen accumulation by L2(25667R). Minor differences in transcript levels between the two strains were identified for the other *glg* genes (Fig. 8C to F) as well as *pgi* and *mrsA_1* (data not shown). Specifically, transcript levels between the strains never exceeded a sevenfold differential for any of the transcripts at the later stages of infection (≥24 h p.i.). We believe that these findings are consistent with the conclusion that glycogen levels, and, hence, its

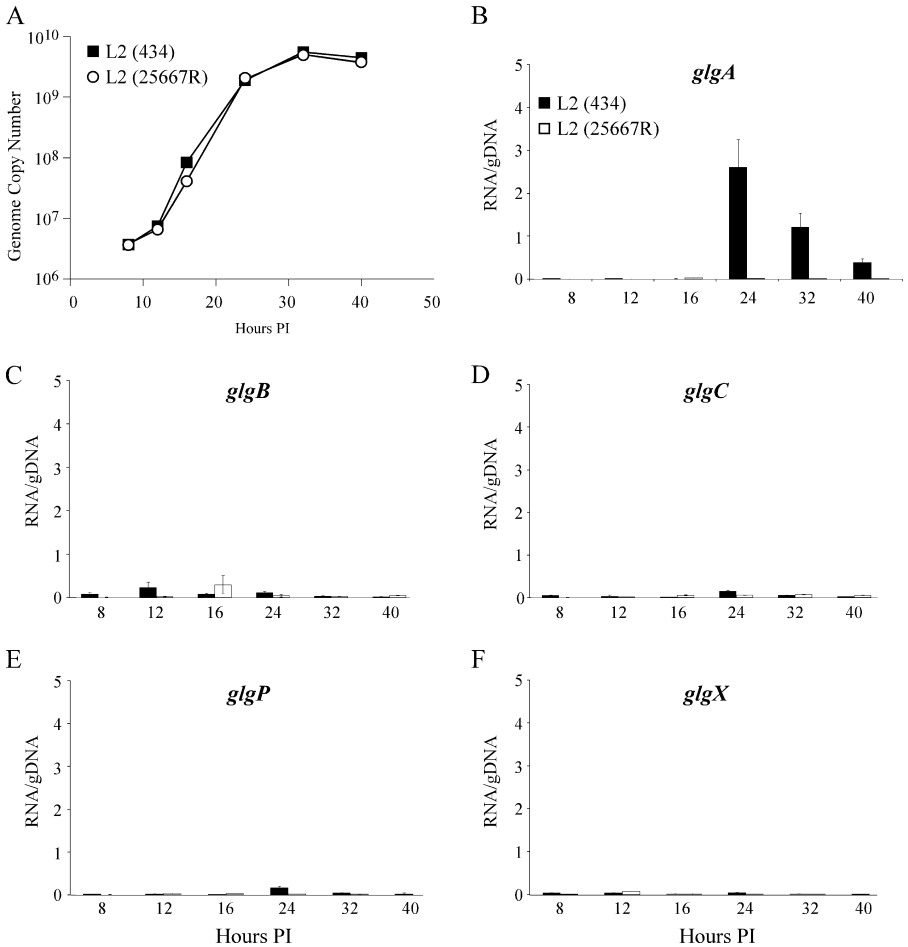

FIG. 8. qRT-PCR of glycogen metabolic genes shows a significant difference in *glgA* expression between L2(434) and L2(25667R). McCoy cells were infected with L2(434) or L2(25667R) (MOI of 1.0) and harvested for RNA and DNA at various times p.i. (PI) (A) Genome copy number was determined using an *rpoB*-specific primer/probe set and TaqMan quantitative PCR. The experiment was performed twice in triplicate. (B to F) Transcript copy number was determined by TaqMan qRT-PCR and normalized to genome copy number (*rpoB*) in matched DNA samples. gDNA, genomic DNA.

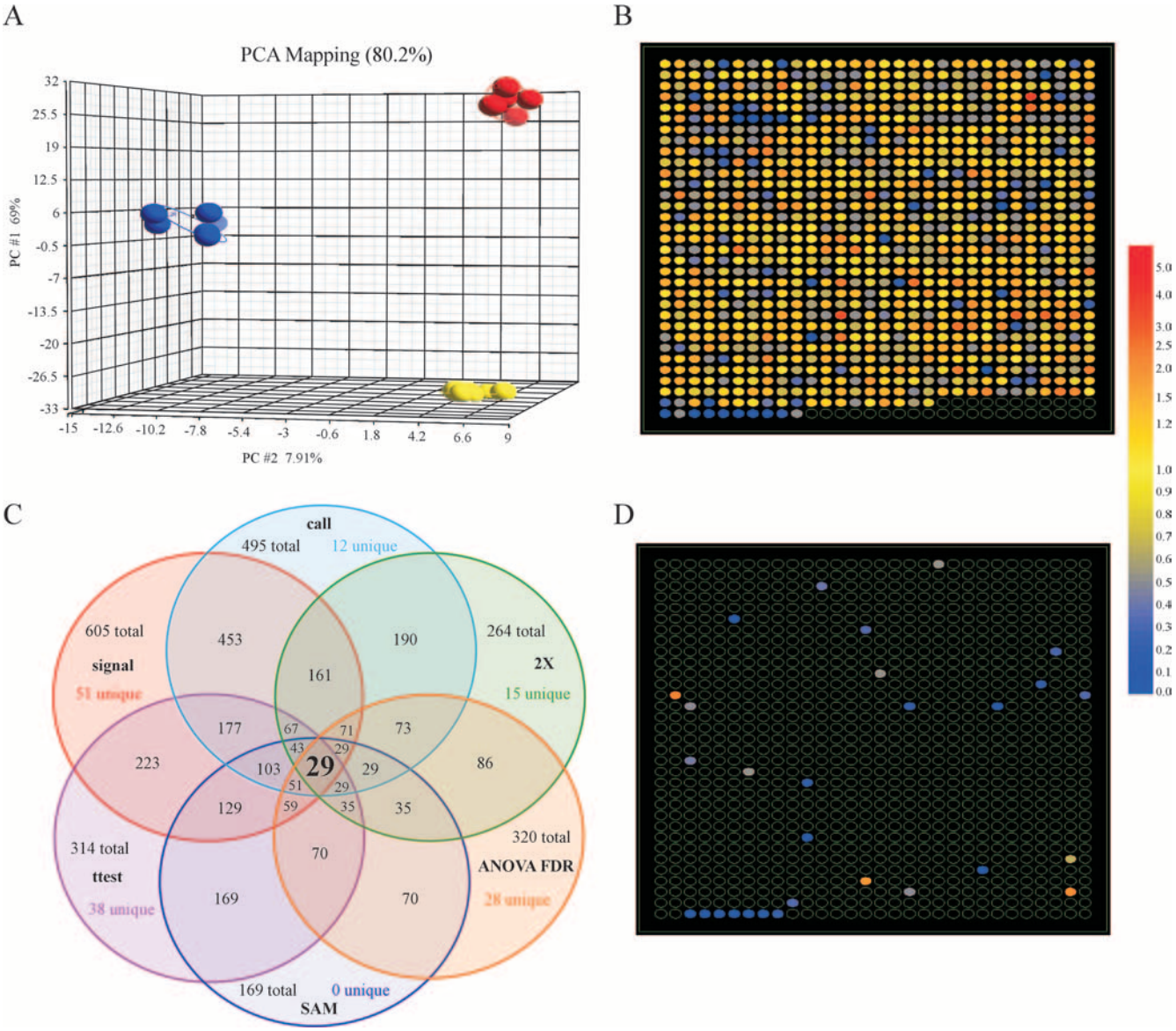

FIG. 9. Microarray transcriptional analysis of strains L2(434) and L2(25667R) 24 h p.i. (A) Principal-component analysis (PCA) of quantile normalized data. Each spot represents all *C. trachomatis* data produced for a single chip, where grouping and separation of replicates and conditions, respectively, are demonstrated [blue, L2(25667R); red, L2(434); yellow, mock). (B) Artificial array image constructed in GeneSpring where each spot represents the differential expression of each chlamydial gene, presented in chromosomal order for all 959 ORF represented on the chip. The vertical scale represents changes in transcript levels of L2(25667R) compared to transcript levels of L2(434). (C) Venn diagram identifying the 29 gene transcripts that passed the statistical and quality tests performed as described in Materials and Methods (signal, signal above background; call, call consistency; 2×, twofold or higher minimum threshold filter; SAM, significance analysis of microarrays; ttest, Student's *t* test). (D) Chromosomal order of the 29 genes identified above (C).

accumulation in the inclusion, are controlled by the level of *glgA* expression. Moreover, the findings support a role for the *C. trachomatis* plasmid in regulating *glgA* expression.

Transcript levels of multiple chromosomal genes are affected by loss of the cryptic plasmid. Our qRT-PCR demonstrated that *glgA* transcript levels were affected by the loss of the cryptic plasmid. We therefore sought to determine whether other chromosomally encoded genes were similarly affected through the use of high-density microarrays. We chose to examine the 24-h p.i. time point, as it was the time point where the highest differential expression of *glgA* was observed and generally coincides with the highest level of transcription for the plasmid-carried genes (5). All results presented were obtained from six independent culture replicates of L2(434)-, L2(25667R)-, and mock-infected McCoy cells. Principal-component analysis demonstrated a high degree of replicate grouping (Fig. 9A). The data from the microarray chips were compiled, and the differential expression results for each chlamydial gene, in the form of change [L2(25667R) versus L2(434)], is presented in chromosomal order (Fig. 9B). After quality filters (upper Venn circles) and multiple statistical algorithms (lower Venn circles) were applied, only 29 genes passed all test criteria (Fig. 9C). The

TABLE 4. Genes demonstrating a twofold or greater transcript differential via microarray analysis[a]

ORF	Gene[c]	Fold change[b]
pL2-06	Hyp	−1,412.96
pL2-07	Hyp	−213.72
pL2-02	Hyp	−98.83
CTL0638	Hyp	−27.66
pL2-05	Hyp	−27.10
CTL0167	*glgA*	−25.28
pL2-03	*dnaB_2*	−11.11
CTL0071	Hyp	−9.88
pL2-04	Hyp	−9.50
CTL0397	Hyp	−9.06
CTL0584	Hyp	−5.29[d]
CTL0187	*mrsA_2*	−5.19
CTL0828	Hyp	−4.81
pL2-08	Hyp	−3.89
CTL0615	*dapA*	−3.00
CTL0633	*pgi*	−2.93
CTL0432	*tauB*	−2.38
CTL0245	*glgB*	−2.17
CTL0222	Hyp	−2.12
CTL0546	*sodM*	−2.10
CTL0272	Hyp	−2.09
CTL0319	*gnd*	−2.03
CTL0618	*dapB*	−2.03
CTL0144	Acetyltransferase	−2.02
CTL0795	*lpxC*	−2.00
CTL0500	*glgP*	−1.97
CTL0762	*ndk*	−1.96
CTL0233	*cpa*	2.09
CTL0589	Hypothetical transcription regulatory protein	2.47

[a] Gene transcripts passing all statistical and quality tests performed as described in Materials and Methods.
[b] Change in L2(25667R) signal compared to L2(434) signal.
[c] Hyp indicates an ORF encoding a hypothetical protein.
[d] Change determined by qRT-PCR, as L2(25667R) signal was not detectable with GeneChip microarrays.

29 genes that met the criteria are displayed in chromosomal order (Fig. 9D) and are listed in Table 4. Transcripts with lower statistical significance are listed in Table S2 in the supplemental material. Of the 29 most significantly differentially expressed genes, 22 were chromosomally encoded genes, while seven were carried on the plasmid. CTL0638 and *glgA* both exhibited >25-fold-decreased expression levels in L2(25667R)- versus L2(434)-infected cells, while all other genes exhibited <10-fold-decreased expression levels. A number of the glycogen metabolic genes, although not all, were also identified as being differentially regulated through our microarray analysis. None of the other glycogen metabolic genes demonstrated differential expression levels comparable to those of *glgA*. Two genes exhibited increased transcripts levels in L2(25667R)- versus L2(434)-infected cells, specifically, CTL0233 (*cpa*) and CTL0589.

To verify our microarray results, 34 qRT-PCR primer and probe sets (see Table S1 in the supplemental material) were employed against 34 *C. trachomatis* mRNAs using the same 24-h p.i. RNA used in our microarray analysis. Seven of the primer/probe sets targeted transcripts from the glycogen metabolic pathway, while 26 were chosen as being in one of two expression classes: high differential or similar expression levels between L2(25667R) and L2(434). A correlation analysis of the changes in a subset of transcripts was conducted by comparing the qRT-PCR and microarray signals. Pearson correlation analysis showed high correlation between the two data sets ($P < 0.001$) (data not shown). We conclude from these results that the cryptic *C. trachomatis* plasmid functions in *trans* to regulate the transcription of multiple chromosomal genes that play an important role in the in vivo pathogenesis of *C. trachomatis* infection.

DISCUSSION

The strong selection for *C. trachomatis* isolates to maintain a 7.5-kb cryptic plasmid in vivo has been a compelling argument for its importance in the pathogenesis of human infection and disease, yet to date, there has been no experimental evidence to support this idea. Here, we have undertaken an extensive investigation of the naturally occurring plasmidless strain *C. trachomatis* L2(25667R) to better define its role as a potential virulence factor. We present evidence suggesting that the plasmid's biological effect on chlamydial pathogenesis is associated with in vivo infection, which enhances the pathogen's ability to colonize and sustain infection in the mouse female genital tract. Furthermore, we have extended these findings to include novel observations that support a functional role for the plasmid-dependent regulation of multiple chromosomal genes. We hypothesize that these genes are virulence factors that are important in *C. trachomatis* infection and disease.

How might plasmid-regulated differences in chromosomal gene expression observed in this work relate to the pathogenesis of in vivo infection? Many of the genes identified encode hypothetical proteins that, in theory, could be critical in establishing in vivo but not in vitro infection, a situation consistent with our findings. As there is no practical genetic system for chlamydiae, it will be difficult to define a functional role for these genes in virulence. A clue to their function may, however, be gleaned from our finding that increased *glgA* transcript levels are associated with the accumulation of glycogen granules in the inclusion matrix.

Glycogen accumulation is not unique to *C. trachomatis*. For example, *Salmonella enterica* serotypes (with the exception of avian-specific variants) also accumulate glycogen. This characteristic has been associated with "niche specialization" (26), similar to *C. trachomatis* species-specific glycogen phenotypes and their respective human host-specific tropisms (17). A role for glycogen in the pathogenesis of *Salmonella* infection was associated with organism survival in tissues rather than colonization or virulence (26). Similarly, *C. trachomatis* is primarily an epitheliotropic pathogen that has the propensity to persist at mucosal surfaces. As such, the mucosa may represent a nutritionally deprived environment where the ability to accumulate glycogen and utilize it as a carbon source is a distinct advantage for chlamydial survival or persistence. Alternatively, glycogen has been proposed to function as a virulence factor in streptococcal infection, where it is thought to be involved in the early stages of cell invasion (58). Indeed, surface polysaccharides have been implicated in *C. trachomatis* species-specific binding to epithelial cells (61). Thus, one might hypothesize that the granules within the inclusion are an extracellular source of ligand that can bind to the EB surface and then serve in the subsequent reinfection or invasion of susceptible host cells through interactions with its cognate host cell receptor.

We initially performed qRT-PCR on all genes predicted to be involved in glycogen metabolism between L2(434) and L2(25667R) and demonstrated that glycogen accumulation in L2(434) directly correlated with a significant increase in the expression levels of *glgA*, a finding consistent with its glycogen-positive phenotype. These results suggest that the plasmid carries either a positive regulator (inducer) of *glgA* transcription or an inhibitor of an unidentified *glgA* repressor (antirepressor). Of the chlamydial genomes sequenced to date, only *C. trachomatis* and *C. muridarum* accumulate glycogen in their mature inclusions (17). Not surprisingly, *C. muridarum* exhibits the highest degree of sequence homology with *C. trachomatis* (39). Some of the more distantly related glycogen-negative chlamydial species either lack a cryptic plasmid (20, 39, 50, 55) or have maintained a plasmid (3, 36, 40) that is more ancestral to the *C. trachomatis* plasmid. Unfortunately, sequence analysis has not revealed a potential plasmid-encoded regulatory factor specific to *C. trachomatis* and *C. muridarum*.

In *Escherichia coli*, the glycogen metabolic genes are clustered together in two adjacent operons (38), and protein expression levels are regulated posttranscriptionally by four different loci, *csrABCD* (14, 44, 53, 60). Conversely, in *C. trachomatis*, the glycogen metabolic genes are scattered throughout the chromosome, and no *csr* homologs have been identified (10, 51, 54). It is critical to demonstrate that the *C. trachomatis* plasmid genes are involved in chromosomal gene expression. In an effort to identify the molecular mechanism of plasmid-associated gene regulation in *C. trachomatis*, we have made a chimeric plasmid between pBR322 and the *C. trachomatis* L2(434) plasmid that is capable of replicating in *E. coli* (data not shown). We plan future surrogate molecular studies employing the chimeric plasmid in a reporter-based assay to identify the mechanism of *C. trachomatis glgA* regulation.

Plasmid control of chromosomally encoded genes would not be unique to *C. trachomatis*. Bai et al. (4) recently identified a protein encoded by the *Yersinia pestis*-specific plasmid pPCPI that bound specifically to upstream regions of a number of chromosomal genes, implicating it as a potential regulatory factor. In addition, enteropathogenic *E. coli* (37) and *Bacillus anthracis* (6) were shown to have chromosomally encoded genes that are regulated by plasmid-encoded loci. Bourgogne et al. (6) further demonstrated that plasmid-mediated regulation elicited changes in the transcript levels of a number of chromosomal genes, a result analogous to what we observed in our chlamydial studies. Not surprisingly, those authors found virulence genes to be differentially regulated in both the *E. coli* and *B. anthracis* plasmid-encoded regulatory mutants.

Our results are in both agreement and disagreement with those recently reported by O'Connell et al. (30) in their studies with *C. muridarum* plasmid-deficient strain CM972. They reported that CM972 produced a small-plaque phenotype whose infection efficiency for the mouse genital tract did not differ from that of its plasmid-positive parent (30). Moreover, they reported that CM972 exhibited no measurable differences in its ability to ascend and replicate in upper genital tract tissues compared to the plasmid-containing parental strain. However, despite its indifferent growth characteristics in the upper genital tract mucosa, CM972 failed to produce significant pathological changes in this tissue, leading O'Connell et al. (30) to conclude that the plasmid affected the induction or augmentation of a damaging innate immune response, the mechanism(s) of which remains undefined. Unfortunately, we could not measure histopathological responses in this study, as LGV, despite its ability to colonize and productively infect the genital mucosa, evokes a very mild and transient acute inflammatory response that does not result in hydrosalpinx (data not shown). Thus, the results of these two studies demonstrate significant in vivo attenuation of plasmidless strains but differ in how attenuation is manifested. Our findings support a role for the *C. trachomatis* plasmid in both initiating and sustaining infection of mucosal epithelial cells. A caveat of our work and conclusions is that the mouse is not the natural host of *C. trachomatis*. Thus, the differences in our findings and those of O'Connell et al. (30) might be reflected in this host-pathogen relationship. As our findings support a role for the *C. trachomatis* plasmid in mediating in vivo infection, a more precise definition of its function in infection and pathogenesis awaits studies in the nonhuman primate host.

ACKNOWLEDGMENTS

We thank Dave Dorward for his expert help with electron microscopy, Anita Mora and Gary Hettrick for their help with the figures, and Kelly Matteson for her help in preparing the manuscript for publication.

This research was supported by the Intramural Research Program of the DIR, NIAID, NIH.

REFERENCES

1. **Albert, T. J., D. Dailidiene, G. Dailide, J. E. Norton, A. Kalia, T. A. Richmond, M. Molla, J. Singh, R. D. Green, and D. E. Berg.** 2005. Mutation discovery in bacterial genomes: metronidazole resistance in *Helicobacter pylori*. Nat. Methods **2:**951–953.
2. **An, Q., G. Radcliffe, R. Vassallo, D. Buxton, W. J. O'Brien, D. A. Pelletier, W. G. Weisburg, J. D. Klinger, and D. M. Olive.** 1992. Infection with a plasmid-free variant chlamydia related to *Chlamydia trachomatis* identified by using multiple assays for nucleic acid detection. J. Clin. Microbiol. **30:**2814–2821.
3. **Azuma, Y., H. Hirakawa, A. Yamashita, Y. Cai, M. A. Rahman, H. Suzuki, S. Mitaku, H. Toh, S. Goto, T. Murakami, K. Sugi, H. Hayashi, H. Fukushi, M. Hattori, S. Kuhara, and M. Shirai.** 2006. Genome sequence of the cat pathogen, Chlamydophilia felis. DNA Res. **13:**15–23.
4. **Bai, G., E. Smith, A. Golubov, J. Pata, and K. A. McDonough.** 2007. Differential gene regulation in *Yersinia pestis* pseudotuberculosis: effects of hypoxia and potential role of a plasmid regulator. Adv. Exp. Med. Biol. **603:**131–144.
5. **Belland, R. J., G. Zhong, D. D. Crane, D. Hogan, D. Sturdevant, J. Sharma, W. L. Beatty, and H. D. Caldwell.** 2003. Genomic transcriptional profiling of the developmental cycle of *Chlamydia trachomatis*. Proc. Natl. Acad. Sci. USA **100:**8478–8483.
6. **Bourgogne, A., M. Drysdale, S. G. Hilsenbeck, S. N. Peterson, and T. M. Koehler.** 2003. Global effects of virulence gene regulators in a *Bacillus anthracis* strain with both virulence plasmids. Infect. Immun. **71:**2736–2743.
7. **Byrne, G. I., and J. W. Moulder.** 1978. Parasite-specified phagocytosis of *Chlamydia psittaci* and *Chlamydia trachomatis* by L and HeLa cells. Infect. Immun. **19:**598–606.
8. **Caldwell, H. D., J. Kromhout, and J. Schachter.** 1981. Purification and partial characterization of the major outer membrane protein of *Chlamydia trachomatis*. Infect. Immun. **31:**1161–1176.
9. **Carlson, J. H., S. Hughes, D. Hogan, G. Cieplak, D. Sturdevant, G. McClarty, H. D. Caldwell, and R. J. Belland.** 2004. Polymorphisms in the *Chlamydia trachomatis* cytotoxin locus associated with ocular and genital isolates. Infect. Immun. **72:**7063–7072.
10. **Carlson, J. H., S. F. Porcella, G. McClarty, and H. D. Caldwell.** 2005. Comparative genomic analysis of *Chlamydia trachomatis* oculotropic and genitotropic strains. Infect. Immun. **73:**6407–6418.
11. **Chiappino, M. L., C. Dawson, J. Schachter, and B. A. Nichols.** 1995. Cytochemical localization of glycogen in *Chlamydia trachomatis* inclusions. J. Bacteriol. **177:**5358–5363.
12. **Comanducci, M., R. Cevenini, A. Moroni, M. M. Giuliani, S. Ricci, V. Scarlato, and G. Ratti.** 1993. Expression of a plasmid gene of *Chlamydia trachomatis* encoding a novel 28 kDa antigen. J. Gen. Microbiol. **139:**1083–1092.
13. **Comanducci, M., S. Ricci, R. Cevenini, and G. Ratti.** 1990. Diversity of the *Chlamydia trachomatis* common plasmid in biovars with different pathogenicity. Plasmid **23:**149–154.
14. **Dubey, A. K., C. S. Baker, T. Romeo, and P. Babitzke.** 2005. RNA sequence and secondary structure participate in high-affinity CsrA-RNA interaction. RNA **11:**1579–1587.

15. **Ellison, D. W., T. R. Clark, D. E. Sturdevant, K. Virtaneva, S. F. Porcella, and T. Hackstadt.** 2008. Genomic comparison of virulent *Rickettsia rickettsii* Shiela Smith and avirulent *Rickettsia rickettsii* Iowa. Infect. Immun. **76:**542–550.
16. **Farencena, A., M. Comanducci, M. Donati, G. Ratti, and R. Cevenini.** 1997. Characterization of a new isolate of *Chlamydia trachomatis* which lacks the common plasmid and has properties of biovar trachoma. Infect. Immun. **65:**2965–2969.
17. **Gordon, F. B., and A. L. Quan.** 1965. Occurrences of glycogen in inclusions of the psittacosis-lymphogranuloma venereum-trachoma agents. J. Infect. Dis. **115:**186–196.
18. **Grayston, J. T., and S. Wang.** 1975. New knowledge of chlamydiae and the diseases they cause. J. Infect. Dis. **132:**87–105.
19. **Iliffe-Lee, E. R., and G. McClarty.** 2000. Regulation of carbon metabolism in *Chlamydia trachomatis*. Mol. Microbiol. **38:**20–30.
20. **Kalman, S., W. Mitchell, R. Marathe, C. Lammel, J. Fan, R. W. Hyman, L. Olinger, J. Grimwood, R. W. Davis, and R. S. Stephens.** 1999. Comparative genomes of *Chlamydia pneumoniae* and *C. trachomatis*. Nat. Genet. **21:**385–389.
21. **Kari, L., W. M. Whitmire, J. H. Carlson, D. D. Crane, N. Reveneau, D. E. Nelson, D. C. Mabey, R. L. Bailey, M. J. Holland, G. McClarty, and H. D. Caldwell.** 2008. Pathogenic diversity among *Chlamydia trachomatis* ocular strains in non-human primates is affected by subtle genomic variations. J. Infect. Dis. **197:**449–456.
22. **Kennedy, A. D., J. A. Willment, D. W. Dorward, D. L. Williams, G. D. Brown, and F. R. Deleo.** 2007. Dectin-1 promotes fungicidal activity of human neutrophils. Eur. J. Immunol. **37:**467.
23. **Li, M., A. E. Villaruz, D. J. Cha, D. E. Sturdevant, and M. Otto.** 2007. Gram-positive three-component antimicrobial peptide-sensing system. Proc. Natl. Acad. Sci. USA **104:**9469–9474.
24. **Magbanua, J. P., B. T. Goh, C. E. Michel, A. Aquirre-Andreasen, S. Alexander, I. Ushiro-Lumb, C. Ison, and H. Lee.** 2007. *Chlamydia trachomatis* variant not detected by plasmid based nucleic acid amplification tests: molecular characterisation and failure of single dose azithromycin. Sex. Transm. Infect. **83:**339–343.
25. **Matsumoto, A., H. Izutsu, N. Miyashita, and M. Ohuchi.** 1998. Plaque formation by and plaque cloning of *Chlamydia trachomatis* biovar trachoma. J. Clin. Microbiol. **36:**3013–3019.
26. **McMeechan, A., M. A. Lovell, T. A. Cogan, K. L. Marston, T. J. Humphrey, and P. A. Barrow.** 2005. Glycogen production by different *Salmonella enterica* serotypes: contribution of functional *glgC* to virulence, intestinal colonization and environmental survival. Microbiology **151:**3969–3977.
27. **Miyashita, N., A. Matsumoto, H. Fukano, Y. Niki, and T. Matsushima.** 2001. The 7.5-kb common plasmid is unrelated to the drug susceptibility of *Chlamydia trachomatis*. J. Infect. Chemother. **7:**113–116.
28. **Miyashita, N., A. Matsumoto, and T. Matsushima.** 2000. In vitro susceptibility of 7.5-kb common plasmid-free *Chlamydia trachomatis* strains. Microbiol. Immunol. **44:**267–269.
29. **Moulder, J. W.** 1982. The relation of basic biology to pathogenic potential in the genus *Chlamydia*. Infection **10**(Suppl. 1)**:**S10–S18.
30. **O'Connell, C. M., R. R. Ingalls, C. W. J. Andrews, A. M. Scurlock, and T. Darville.** 2007. Plasmid-deficient *Chlamydia muridarum* fail to induce immune pathology and protect against oviduct disease. J. Immunol. **176:**4027–4034.
31. **O'Connell, C. M., and K. M. Nicks.** 2006. A plasmid-cured *Chlamydia muridarium* strain displays altered plaque morphology and reduced infectivity in cell culture. Microbiology **152:**1601–1607.
32. **Palazollo-Balance, A. M., M. L. Reniere, K. R. Braughton, D. E. Sturdevant, M. Otto, B. N. Kreiswirth, E. P. Skaar, and F. R. Deleo.** 2008. Neutrophil microbicides induce a pathogen survival response in community-associated methicillin-resistant *Staphylococcus aureus*. J. Immunol. **180:**500–509.
33. **Palmer, L., and S. Falkow.** 1986. A common plasmid of *Chlamydia trachomatis*. Plasmid **16:**52–62.
34. **Perry, L. L., K. Feilzer, and H. D. Caldwell.** 1997. Immunity to *Chlamydia trachomatis* is mediated by T helper 1 cells through IFN-γ-dependent and -independent pathways. J. Immunol. **158:**3344–3352.
35. **Peterson, E. M., B. A. Markoff, J. Schachter, and L. M. de la Maza.** 1990. The 7.5-kb plasmid present in *Chlamydia trachomatis* is not essential for the growth of this microorganism. Plasmid **23:**144–148.
36. **Pickett, M. A., J. S. Everson, P. J. Pead, and I. N. Clarke.** 2005. The plasmids of *Chlamydia trachomatis* and *Chlamydophila pneumoniae* (N16): accurate determination of copy number and the paradoxical effect of plasmid-curing agents. Microbiology **151:**893–903.
37. **Porter, M. E., P. Mitchell, A. J. Roe, A. Free, D. G. Smith, and D. L. Gally.** 2004. Direct and indirect transcriptional activation of virulence genes by an AraC-like protein, PerA from enteropathogenic *Escherichia coli*. Mol. Microbiol. **54:**1117–1133.
38. **Preiss, J.** 1996. Regulation of glycogen synthesis, p. 1015–1023. *In* F. C. Neidhart, R. Curtiss III, J. L. Ingraham, E. C. C. Lin, K. B. Low, B. Magasanik, W. S. Reznikoff, M. Riley, M. Schaechter, and H. E. Umbarger (ed.), *Escherichia coli* and *Salmonella*: cellular and molecular biology, 2nd ed. ASM Press, Washington, DC.
39. **Read, T. D., R. C. Brunham, C. Shen, S. R. Gill, J. F. Heidelberg, O. White, E. K. Hickey, J. Peterson, T. Utterback, K. Berry, S. Bass, K. Linher, J. Weidman, H. Khouri, B. Craven, C. Bowman, R. Dodson, M. Gwinn, W. Nelson, R. DeBoy, J. Kolonay, G. McClarty, S. L. Salzberg, J. Eisen, and C. M. Fraser.** 2000. Genome sequences of *Chlamydia trachomatis* MoPn and *Chlamydia pneumoniae* AR39. Nucleic Acids Res. **28:**1397–1406.
40. **Read, T. D., G. S. Myers, R. C. Brunham, W. C. Nelson, I. T. Paulsen, J. F. Heidelberg, E. Holtzapple, H. Khouri, N. B. Federova, H. A. Carty, L. A. Umayam, D. H. Haft, J. Peterson, M. J. Beanan, O. White, S. L. Salzberg, R. Hsia, G. McClarty, R. G. Rank, P. M. Bavoil, and C. M. Fraser.** 2003. Genome sequence of *Chlamydophila caviae* (*Chlamydia psittaci* GPIC): examining the role of niche-specific genes in the evolution of the Chlamydiaceae. Nucleic Acids Res. **31:**2134–2147.
41. **Reed, L. J., and H. Muench.** 1938. A simple method of estimating 50 percent endpoints. Am. J. Hyg. **27:**493–497.
42. **Ricci, S., R. Cevenini, M. Comanducci, G. Ratti, and V. Scarlato.** 1993. Transcriptional analysis of the *Chlamydia trachomatis* plasmid pCT identifies temporarily regulated transcripts. Mol. Gen. Genet. **237:**318–326.
43. **Ricci, S., G. Ratti, and V. Scarlato.** 1995. Transcriptional regulation in the *Chlamydia trachomatis* pCT plasmid. Gene **154:**93–98.
44. **Romeo, T., M. Gong, M. Y. Liu, and A. M. Brun-Zinkernagel.** 1993. Identification and molecular characterization of *csrA*, a pleiotropic gene from *Escherichia coli* that affects glycogen biosynthesis, gluconeogenesis, cell size, and surface properties. J. Bacteriol. **175:**4744–4755.
45. **Sabet, S. F., J. Simmons, and H. D. Caldwell.** 1984. Enhancement of *Chlamydia trachomatis* infectious progeny by cultivation of HeLa 229 cells treated with DEAE-dextran and cycloheximide. J. Clin. Microbiol. **20:**217–222.
46. **Schachter, J.** 1978. Chlamydial infections (first of three parts). N. Engl. J. Med. **298:**428–434.
47. **Schachter, J.** 1978. Chlamydial infections (second of three parts). N. Engl. J. Med. **298:**490–495.
48. **Schachter, J., and C. R. Dawson.** 1978. Human chlamydial infections, p. 83–88. PSG Publishing Co., Inc., Littleton, MA.
49. **Schachter, J., and A. O. Osoba.** 1983. Lymphogranuloma venereum. Br. Med. Bull. **39:**151–154.
50. **Shirai, M., H. Hirakawa, M. Kimoto, M. Tabuchi, F. Kishi, K. Ouchi, T. Shiba, K. Ishii, M. Hattori, S. Kuhara, and T. Nakazawa.** 2000. Comparison of whole genome sequences of *Chlamydia pneumoniae* J138 from Japan and CWL029 from USA. Nucleic Acids Res. **28:**2311–2314.
51. **Stephens, R. S., S. Kalman, C. Lammel, J. Fan, R. Marathe, L. Aravind, W. Mitchell, L. Olinger, R. L. Tatusov, Q. Zhao, E. V. Koonin, and R. W. Davis.** 1998. Genome sequence of an obligate intracellular pathogen of humans: *Chlamydia trachomatis*. Science **282:**754–759.
52. **Stothard, D. R., J. A. Williams, B. Van der Pol, and R. B. Jones.** 1998. Identification of a *Chlamydia trachomatis* serovar E urogenital isolate which lacks the cryptic plasmid. Infect. Immun. **66:**6010–6013.
53. **Suzuki, K., P. Babitzke, S. R. Kushner, and T. Romeo.** 2006. Identification of a novel regulatory protein (CsrD) that targets the global regulatory RNAs CsrB and CsrC for degradation by RNase E. Genes Dev. **20:**2605–2617.
54. **Thomson, N. R., M. T. Holden, C. Carder, N. Lennard, S. J. Lockey, P. Marsh, P. Skipp, C. D. O'Conner, I. Goodhead, H. Norbertzake, B. Harris, D. Ormond, R. Rance, M. A. Quail, J. Parkhill, R. S. Stephens, and I. N. Clarke.** 2008. *Chlamydia trachomatis*: genome sequence analysis of lymphogranuloma venereum isolates. Genome Res. **18:**161–171.
55. **Thomson, N. R., C. Yeats, K. Bell, M. T. Holden, S. D. Bentley, M. Livingstone, A. M. Cerdeno-Tarraga, B. Harris, J. Doggett, D. Ormond, K. Mungall, K. Clarke, T. Feltwell, Z. Hance, M. Sanders, M. A. Quail, C. Price, B. G. Barrell, J. Parkhill, and D. Longbottom.** 2005. The *Chlamydophila abortus* genome sequence reveals an array of variable proteins that contribute to interspecies variation. Genome Res. **15:**629–640.
56. **Todd, W. J., and H. D. Caldwell.** 1985. The interaction of *Chlamydia trachomatis* with host cells: ultrastructural studies of the mechanism of release of a biovar II strain from HeLa 229 cells. J. Infect. Dis. **151:**1037–1044.
57. **Tusher, V. G., R. Tibshirani, and G. Chu.** 2001. Significance analysis of microarrays applied to the ionizing radiation response. Proc. Natl. Acad. Sci. USA **98:**5116–5121.
58. **van Bueren, A. L., M. Higgins, D. Wang, R. D. Burke, and A. B. Boraston.** 2007. Identification and structural basis of binding to host lung glycogen by streptococcal virulence factors. Nat. Struct. Mol. Biol. **14:**76–84.
59. **Virtaneva, K., S. F. Porcella, M. R. Graham, R. M. Ireland, C. A. Johnson, S. M. Ricklefs, I. Babar, L. D. Parkins, R. A. Romero, G. J. Corn, J. R. Bailey, M. J. Parnell, and J. M. Musser.** 2005. Longitudinal analysis of the group A Streptococcus transcriptome in experimental pharyngitis in cynomolgus macaques. Proc. Natl. Acad. Sci. USA **102:**9014–9019.
60. **Yang, H., M. Y. Liu, and T. Romeo.** 1996. Coordinate genetic regulation of glycogen catabolism and biosynthesis in *Escherichia coli* via the CsrA gene product. J. Bacteriol. **178:**1012–1017.
61. **Zhang, J. P., and R. S. Stephens.** 1992. Mechanism of *C. trachomatis* attachment to eukaryotic host cells. Cell **69:**861–869.

Editor: R. P. Morrison